Spring 5-1-2017

Characterization of Novel Cannabinoid Receptor 2-Selective Agonists at the Biochemical and Cellular Levels: Leads for Therapeutic Agents

Ashley M. Hine
University of Connecticut - Storrs, ashley.hine@uconn.edu

Characterization of Novel Cannabinoid Receptor 2-Selective Agonists at the Biochemical and Cellular Levels: Leads for Therapeutic Agents

Ashley M. Hine

An Honors Scholar Thesis
Submitted in Partial Fulfillment of the
Requirements for the Degree of
Bachelor of Science

May 2017

University of Connecticut

Department of Physiology and Neurobiology
Department of Molecular and Cell Biology

Thesis Advisor: Debra A. Kendall, PhD

Honors Advisor: Joseph F. Crivello, PhD

ABSTRACT

Putative cannabinoid receptor 2 (CB_2)-selective agonists were identified from a library of commercially available compounds via inhibition of cAMP accumulation in high throughput screening. Binding affinity and receptor subtype selectivity were assessed using heterologous competition binding assays against the known cannabinoid orthosteric ligand CP55940. Test compounds ASX0152383 and CSC003141 preferentially bound to CB_2, with no detection of binding to CB_1 up to 1 μM. CMB038865 exhibited nearly 100-fold selectivity for CB_1 over CB_2, while CZ000026 bound non-preferentially to both receptors in the low micromolar range. To determine the extent of G protein coupling, GTPγS binding assays were performed. Dose-dependent increases in binding of the nonhydrolyzable GTP analog to Gα subunits were induced by all test compounds. G protein-mediated MAPK signaling downstream of high affinity compounds was assessed by measuring ERK1/2 phosphorylation in the presence and absence of pertussis toxin (PTX). Activation induced by ASX015283 agonism at CB_2 resulted in ERK 1/2 phosphorylation which was abrogated by PTX, indicating $G_{i/o}$ protein-dependence. Interestingly, CMB038865 agonism at CB_1 resulted in low levels of ERK phosphorylation and signaling was not abrogated by PTX. However, CMB038665 agonism at CB_2 resulted in robust levels of ERK phosphorylation in a PTX-sensitive manner, indicative of $G_{i/o}$ protein-dependent signaling. These results indicate CMB038865 is a partially selective CB_1 agonist potentially biased towards G protein signaling pathways, while ASX015283 and CSC003141 are CB_2-selective agonists that may possess therapeutic potential for the treatment of chronic pain and inflammation without the psychoactive effects concomitant with activation of CB_1 receptors in the central nervous system.

ACKNOWLEDGEMENTS

First and foremost, I thank my thesis advisor, Dr. Debra Kendall, for providing me with the opportunity to work in her lab. Without her taking a chance on me, I would have never discovered the exhilaration of scientific pursuit. I would also like to extend my thanks to Dr. Andrew Alt, formerly of Bristol-Myers Squibb, as well as Dr. Neil Burford for their assistance with the project at large and intellectual contribution.

Additionally, I thank all of the members of the Kendall Laboratory for scientific discussion and invaluable camaraderie, with particular gratitude to Dr. Yu-Hsien “Rex” Liao. It was truly a pleasure to work alongside him and learn from him. I thank him for his infinite patience, words of wisdom provided in times most necessary, and life lessons that I will reflect back on in years to come. I would also like to thank Caitlin Jagla for assistance with image quantification, gladly proofreading many drafts, and for her friendship.

I thank the UConn Honors Program for enriching my undergraduate experience with exceptional professors, stimulating coursework, and cutting-edge research.

Lastly, I sincerely thank my family and friends for their continuous and unconditional support, patience, and encouragement throughout the foundation of my academic journey. I dedicate this honors scholar thesis as the culmination of my undergraduate career and product of success as a first-generation student to my mother, who has been my primary proponent and inspires me to persist in the face of adversity.

This research was funded by a Presidential Scholar enrichment award from the University of Connecticut Office of National Scholarships and Fellowships (to A.M.H.) and the National Institutes of Health (to D.A.K).

TABLE OF CONTENTS

1. BACKGROUND AND SIGNIFICANCE.....1

1.1 G Protein-Coupled Receptors and Clinical Significance 1

1.2 GPCR Structure..... 1

1.3 GPCR Signal Transduction 2

1.4 The Cannabinoid Receptors..... 2

1.5 Orthosteric Activation and Receptor States..... 3

1.6 Cannabinoid Receptor Family Ligands..... 4

1.6.1 Endocannabinoids 4
1.6.2 Phytocannabinoids 4
1.6.3 Synthetic Cannabinoids..... 4

1.7 Putative Novel CB_2 - Selective Agonists..... 5

2. MATERIALS AND METHODS.....9

2.1 Compounds. 9

2.2 CB_1 and CB_2 Expression and Membrane Preparation. 9

2.3 Saturation Radioligand Binding. 10

2.4 Radioligand Binding..... 10

2.5 Guanosine 5'-O-(3-Thio)Triphosphate (GTPγS) Binding. 10

2.6 Immunoblotting Studies for ERK1/2 Phosphorylation..... 11

2.7 Data Analysis and Image Quantification..... 12

3. RESULTS.....13

3.1 Saturation binding isotherms. 13

3.2 ASX015283 and CSC003141 exhibit preferential binding to CB_2. 14

3.3 CMB038865 exhibits nearly 100X selectivity for CB_1. 15

3.4 CZ000026 does not exhibit receptor subtype selectivity. 16

3.5 Dose-dependent GTPγS binding is elicited by all test compounds. 17

3.6 Extracellular signal-regulated kinase phosphorylation studies. 18

4. DISCUSSION 22

REFERENCES.....26

1. BACKGROUND AND SIGNIFICANCE

1.1 G Protein-Coupled Receptors and Clinical Significance

G protein-coupled receptors (GPCRs) are seven-transmembrane (7-TM) domain proteins that are abundant and a physiologically instrumental receptor superfamily in the human body. Upon ligand binding, GPCRs transduce extracellular signals across the biological membrane to elicit cellular responses. GPCR ligands are diverse in nature and include photons, odorant molecules, growth factors, hormones, peptides, small molecules, and neurotransmitters. This multiplicity of ligands facilitates the diverse role of GPCRs in significant physiological processes including hormone signaling, homeostatic mechanisms, behavioral modulation, mediation of the senses including vision, gustation, olfaction, autonomic nervous system transmission and immune regulation. This diversity leads to critical involvement in numerous pathologies, and GPCRs are thus an attractive target for drug discovery (Rosenbaum et al., 2009).

1.2 GPCR Structure

GPCRs are divided into six subclasses (A-F) based on functional similarity and sequence homology. Structural commonalities across GPCR classes include the characteristic 7-TM α-helices consisting of approximately 25-35 predominantly hydrophobic amino acid residues each, an extracellular amino terminus, and an intracellular carboxyl terminus (Gilchrist, 2010). In addition, three intracellular (IC1-3) and three extracellular (EC1-3) loops alternately connect the helices. Particularly in the case of class A GPCRs, which are exemplified by the prototypical rhodopsin, the extracellular loops and the top portions of the TM domains are thought to form pockets to which ligands bind the receptor while the

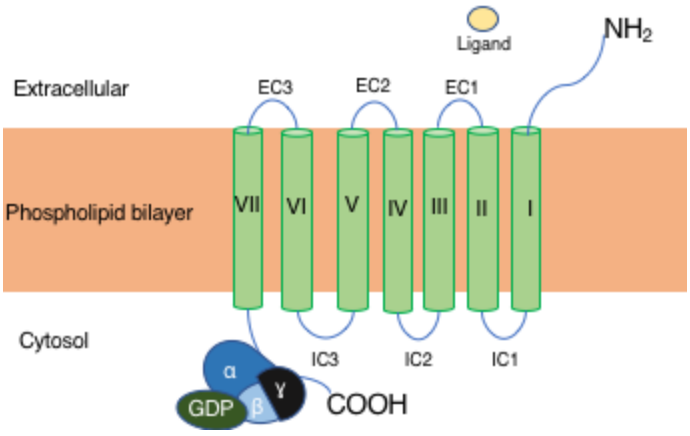

Figure 1. Structural schematic of a G protein-coupled receptor in the inactivated GDP-bound state.

intracellular regions are thought to interact with downstream effectors including guanine nucleotide-binding proteins (heterotrimeric G proteins) and β-arrestins (Wootten et al., 2013).

1.3 GPCR Signal Transduction

Upon ligand binding, the GPCR undergoes a conformational change resulting in structural rearrangement of the α-helices and receptor activation. Intracellular heterotrimeric G proteins consisting of Gα, Gβ and Gγ subunits also become activated. This activation triggers the dissociation of guanine diphosphate (GDP), which is bound to the inactive G protein, to facilitate the binding of guanine triphosphate (GTP) to the Gα subunit (the active state). The Gα subunit bound to GTP dissociates from the βγ complex and can subsequently initiate downstream signaling events. For a comprehensive review on GPCR signaling, see Whalen et al., 2011.

1.4 The Cannabinoid Receptors

The cannabinoid receptors are among the class A rhodopsin-like GPCR subfamily. There are two canonical cannabinoid receptors, cannabinoid receptor one (CB_1) and cannabinoid receptor two (CB_2), although a recently deorphanized GPCR, GPR55, has been proposed as a putative cannabinoid receptor (Shore and Reggio, 2015).

Both CB_1 and CB_2 predominantly couple to pertussis toxin-sensitive $G_{i/o}$ proteins to inhibit adenylate cyclase, the enzyme responsible for the conversion of ATP into cAMP. However, CB_1 under certain circumstances can couple to G_s proteins and activate adenylate cyclase (Turu and Hunyady, 2010).

CB_1 is primarily associated with the central nervous system (CNS) and predominantly located on presynaptic terminals of neurons within regions of the brain including the hippocampus, cerebral cortex, and cerebellum. Within these regions, activation of CB_1, the most abundant and ubiquitous GPCR in the CNS, inhibits neurotransmitter release

via retrograde signaling mechanisms (Mikasova et al., 2008). Secondarily, CB_1 is also located peripherally in the gastrointestinal tract, reproductive tract and endocrine tissue.

CB_2 is predominantly located in peripheral and immune tissue including hematopoietic cells such as lymphocytes, natural killer cells and macrophages. CB_2 has also been characterized in neuroglial tissue of the central nervous system including resident macrophages of the brain, microglia, and is associated with inflammation (Amenta et al., 2014). Furthermore, activation of CB_2 has been implicated in dampening the replication of human immunodeficiency virus (HIV) in macrophages (Persidsky et al., 2015).

1.5 Orthosteric Activation and Receptor States

GPCRs are canonically activated via ligand binding at the orthosteric site, which is identified as the site of endogenous ligand binding. However, some receptor populations contain one or more additional, topographically distinct, sites for allosteric modulator binding. CB_1 is one such receptor, containing at least one allosteric site. However, this work is primarily focused on orthosteric agonists of CB_2, which does not have any known allosteric sites.

Some GPCRs exhibit constitutive activity, such as the cannabinoid receptors. Constitutively active receptors are present in the active state without the presence of bound ligand, leading to a basal level of activity and downstream signaling. Receptor activity is differentially modified from the basal level by the binding of various orthosteric ligand types. Agonists promote the active conformation of the receptor to varying extents. Full agonists elicit a maximal biological response, while partial agonists cannot elicit as large an effect

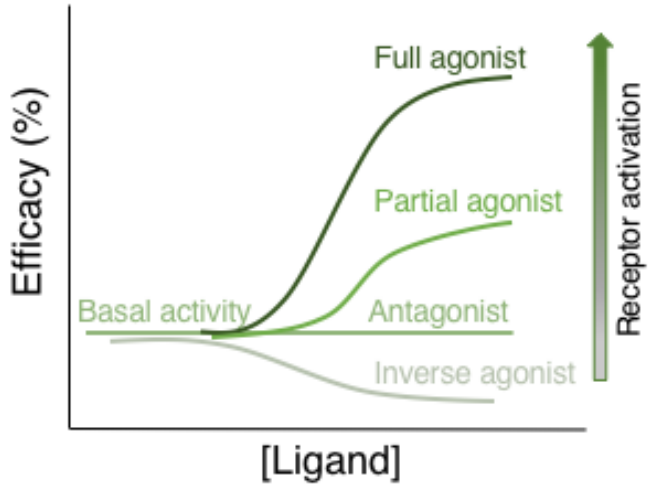

Figure 2. Differential levels of GPCR activation.

on the same receptors. Inverse agonists promote the inactive state of the receptor and reduce the number of receptors in the active conformation. Antagonists do not elicit a change in the receptor state and have no effect on signaling. Although antagonist binding blocks the orthosteric site, receptor activity remains at basal level.

1.6 Cannabinoid Receptor Family Ligands

The cannabinoid receptors bind three subclasses of classical neuromodulatory lipids: endocannabinoids, phytocannabinoids and synthetic cannabinoids. Ligands of all three subclasses are generally hydrophobic molecules that bind the orthosteric site of the receptor.

1.6.1 Endocannabinoids

The endocannabinoids are endogenous omega-6 fatty acid-derived ligands produced in the brain. Along with the cannabinoid receptors, the endocannabinoids and the enzymes responsible for catalyzing reactions involved in their synthesis and degradation constitute the endocannabinoid system. The two major endocannabinoids are N-arachidonoylethanolamine, or anandamide (AEA) and 2-arachidonoylglycerol (2-AG).

1.6.2 Phytocannabinoids

Phytocannabinoids are plant-derived ligands. The major ligand of this class is Δ^9-tetrahydrocannabinol (Δ^9-THC; derived from *Cannabis sativa*), the main psychoactive component of marijuana and a partial agonist of both CB_1 and CB_2. Cannabidiol (CBD) is another major phytocannabinoid derived from *Cannabis sativa*. CBD may bind to both CB_1 and CB_2, but at concentrations in the micromolar range, and is thus considered to possess low affinity for both receptors. In contrast to Δ^9-THC, CBD is considered to be non-psychotrophic (Pertwee, 2008).

1.6.3 Synthetic Cannabinoids

The third ligand subclass includes synthetic endocannabinoids, which are generally modified structures of endocannabinoids and phytocannabinoids optimized as potential small molecule drugs. CP55940 ((1*R*,3*R*,4*R*)-3-[2-hydroxy-4-(1,1-dimethylheptyl)phenyl]-4-(3- hydroxypropyl)cyclohexan-1-ol) is a full agonist at both CB_1 and CB_2 with affinities in the low nanomolar range (i.e. < 5 nM). SR141716A (5-(4-chlorophenyl)-1-(2,4-dichloro-phenyl)-4-methyl-*N*-(piperidin-1-yl)-1*H*-pyrazole-3-carboxamide) is an

antagonist of CB_1 that was clinically approved and marketed in Europe as the anti-obesity drug rimonabant. Within a few years of approval, the drug was withdrawn from the market due to psychiatric side effects including major depression, anxiety, and suicidal thoughts in patient populations (Erdozain et al., 2012).

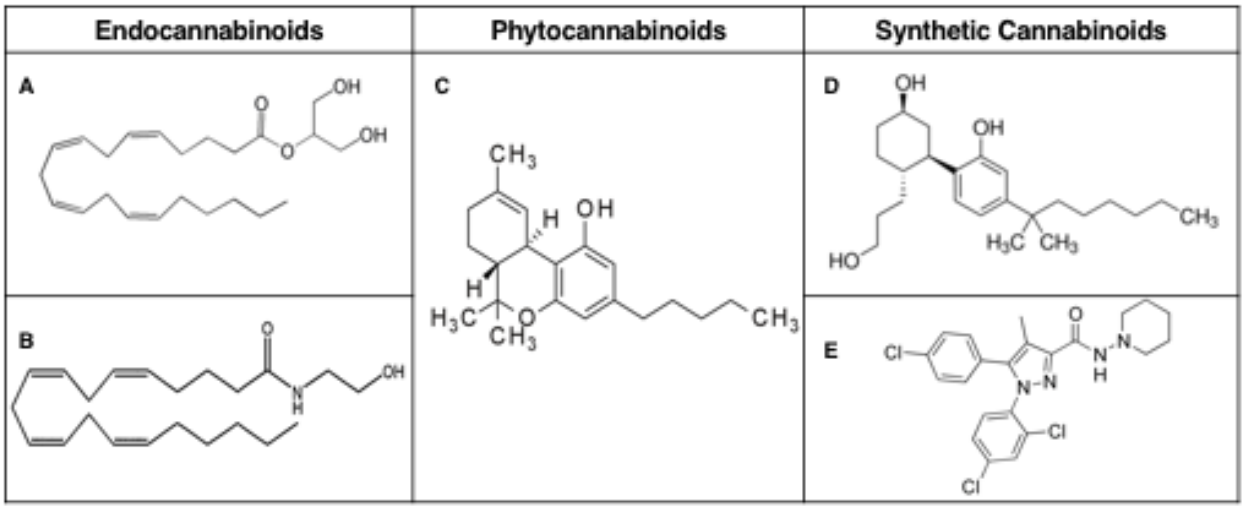

Figure 3. Chemical structures of cannabinoid receptor ligands: (A) 2-AG and (B) AEA are endocannabinoids, (C) Δ^9-THC is a phytocannabinoid, and (D) CP55940 and (E) SR141716A are synthetic cannabinoids. The latter is an inverse agonist while all others shown are agonists.

1.7 Putative Novel CB_2 - Selective Agonists

Commercially available putative cannabinoid receptor 2-selective agonists were identified as hits in a high throughput screen (HTS) from a library of approximately 40,000 compounds. Receptor selectivity was assessed by using CHO-K1 cells transfected with CB_2 relative to the null strain. Ligands were identified based on inhibition of cAMP accumulation. Previously synthesized for other purposes, these small molecules have been further assessed for their selectivity for CB_2 and effects on downstream signaling in this study.

ASX015283 (2-(7-oxo-2,3-dihydro-7H-furo[3,2-g]chromen-2-yl)propan-2-yl 2,4-dichlorobenzoate; Figure 4A) is a modification of parent compound, felamidin (2-[(2S)-7-oxo-2,3-dihydrofuro[3,2-g]chromen-2-yl]propan-2-yl benzoate; Figure 4B). ASX015283 has been synthetically modified from felamidin with the addition of two chloro-substituents on the distal benzene ring. The parent compound, felamidin, was one of

2,000 biologically active compounds from The Spectrum Collection compound library by MicroSource Discovery Systems. Initial HTS of this library was performed for inhibitors of 6-phosphogluconate dehydrogenase (6-PGD), an enzyme responsible for catalyzing the conversion of 6-phosphogluconate into ribulose 5-phosphate during the oxidative phase of the pentose phosphate pathway. Felamidin was found to be biologically active as a 6-PGD inhibitor and shown to affect cancer cell metabolism in animal studies by inhibiting cell proliferation and tumor growth (Lin et al., 2015). Additionally, felamidin was found to inhibit tumor cell replication with an EC_{50} of 11.6 μM in a test for cytotoxicity against A549 non-small cell lung cancer cells (Rosselli et al., 2009).

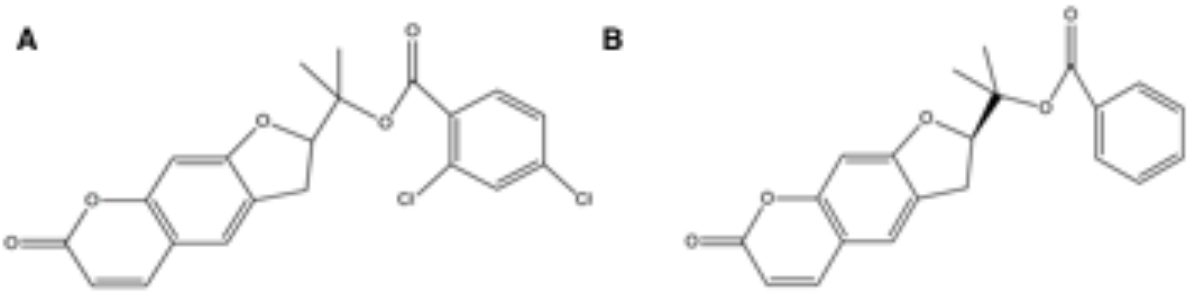

Figure 4. Chemical structures of (A) test compound ASX015283 (molecular weight: 419. 265 g/mol), and (B) parent compound, felamidin (molecular weight: 350.37 g/mol).

CSC003141(4-(tert-butyl)-N-(2,2,2-trichloro-1-(4-methylpiperidin-1-yl)ethyl)benzamide; Figure 5A) was tested for inhibition of HIV-1 RNase in a fluorescence-based HTS, but found to be inactive. However, a structurally similar compound, 4-fluoro-*N*-[2,2,2-trichloro-1-(4-morpholinyl)ethyl]-benzamide (Figure 5B), was identified from a compound library at The Scripps Research Institute Molecular Screening Center as biologically active in HTS of multiple class A rhodopsin-like GPCRs including the neuropeptide Y receptor Y1 (NPY-Y1) and the human muscarinic cholinergic receptor (hM1). This small molecule differs from test compound CSC003141 in that a methyl group has been removed and an oxygen has been substituted into the heteroatom ring while a fluoro- substituent has replaced the bulky tert-butyl group. This compound was active as a NPY-Y1 antagonist, and such molecules have therapeutic implications in appetite and circadian rhythms (Ishii et al., 2007). It was also found to be a human muscarinic cholinergic hM1 agonist with clinical

implications in the treatment of Alzheimer's disease and schizophrenia (Matucci et al., 2016).

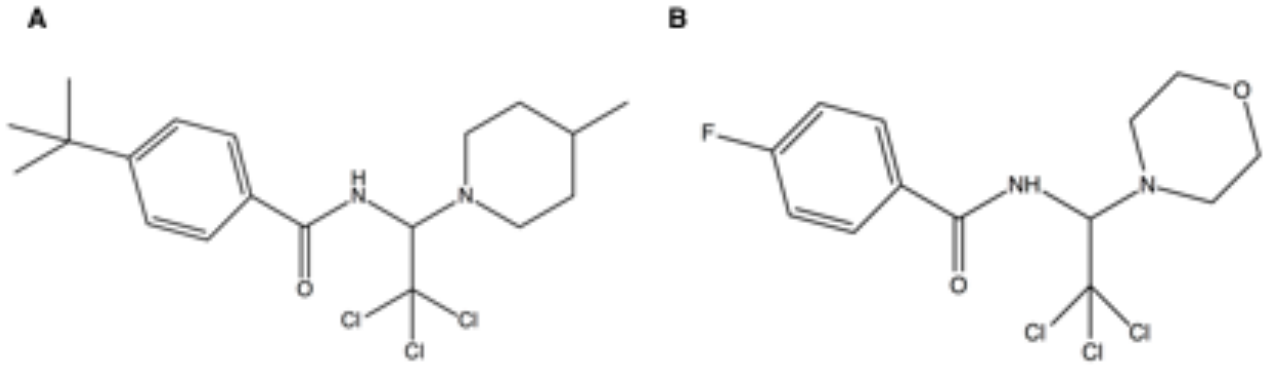

Figure 5. Chemical structures of test compound CSC003141 (molecular weight: 405.799 g/mol) (A), and structurally similar compound (4-fluoro-*N*-[2,2,2-trichloro-1-(4-morpholinyl)ethyl]-benzamide) that is biologically active as a GPCR class A ligand (B).

CMB038865 (1-(indoline-1-carbonyl)-4,7,7-trimethyl-2-oxabicyclo[2.2.1]heptan-3-one; Figure 6A) is structurally related to compound CHEMBL2338187 (PubChem ID; Figure 6B) with an adamantane ring modification and agonist activity at CB_2 identified in cAMP and β-arrestin recruitment assays (Nettekoven et al., 2013).

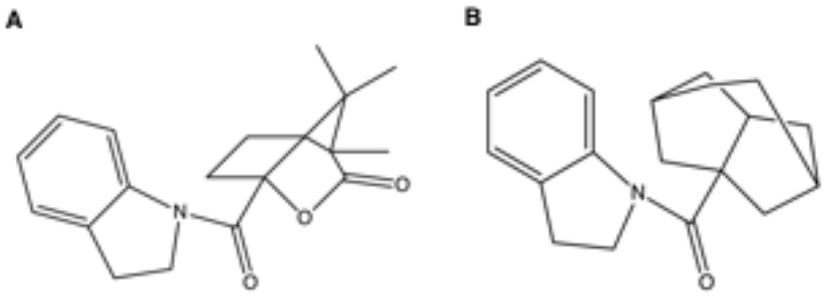

Figure 6. Chemical structure of test compound CMB038865 (molecular weight: 299.37 g/mol) (A), and similar structure CHEMBL2338187 (molecular weight: 267.372 g/mol) (B).

CZ000026 (N2,N3-diphenylquinoxaline-2,3-diamine; Figure 7) has been patented as a farnesoid X receptor (FXR) antagonist (Houze et al., U.S. Patent 7,511,043, 2009). FXR antagonists are potential therapeutics for the treatment of hypercholesterolemia. By controlling the rate-limiting enzyme involved in metabolism of cholesterol to bile acids, cholesterol

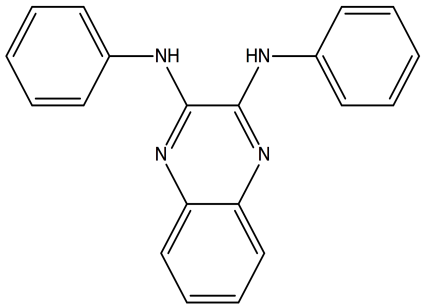

Figure 7. Chemical structure of test compound CZ000026 (molecular weight 312. 376 g/mol).

7 alpha-hydroxylase (CYP7A1), it is possible to modulate FXR-mediated gene expression (Sepe et al., 2016).

2. MATERIALS AND METHODS

2.1 Compounds.

Test compounds ASX01583 (2-(7-oxo-2,3-dihydro-7H-furo[3,2-g]chromen-2-yl)propan-2-yl 2,4-dichlorobenzoate), CSC003141 (4-(tert-butyl)-N-(2,2,2-trichloro-1-(4-methylpiperidin-1-yl)ethyl)benzamide), CMB038865 (1-(indoline-1-carbonyl)-4,7,7-trimethyl-2-oxabicyclo[2.2.1]heptan-3-one), and CZ000026 (N2,N3-diphenylquinoxaline-2,3-diamine) were obtained from Bristol-Myers Squibb (Wallingford, CT) as hits from high throughput screening conducted for CB_2-selective agonists. Briefly, assays to assess inhibition of cAMP accumulation were performed in duplication using Chinese hamster ovary-K1 (CHO-K1) cells both expressing and lacking CB_2, with the output of half maximal effective concentration (EC_{50}) values. 10 mM stock concentrations of compound were prepared in dimethyl sulfoxide (DMSO) with particular attention to air exposure and were subsequently serially diluted.

2.2 CB_1 and CB_2 Expression and Membrane Preparation.

Human embryonic kidney 293T (HEK293T) cells (ATCC, Manassas, VA) were seeded at a density of approximately 1.0×10^6 cells per 100 mm dish in Dulbecco's modified Eagle's medium (DMEM) supplemented with 10% fetal bovine serum (FBS) and 3.5 mg/ml glucose at 37°C in 5% CO_2. For transient expression of receptors, after approximately twenty-four hours, cells were transfected with 5-10 μg CB_1 or CB_2 cloned into pcDNA 3.1 using the calcium phosphate precipitation method (Chen and Okayama, 1987) or Lipofectamine 2000 (Invitrogen, Carlsbad, CA). Approximately twenty-four hours post-transfection, cells were harvested and washed twice with phosphate-buffered saline (PBS; 137 mM NaCl, 2.7 mM KCl, 10 mM Na_2HPO_4,1.8 mM KH_2PO_4, pH 7). After resuspension in PBS supplemented with mammalian protease inhibitor cocktail containing 4-(2-aminoethyl)benzenesulfonyl fluoride (AEBSF), pepstatin A, E-64, bestatin, leupeptin, and aprotinin (Sigma, St. Louis, MO), cells were lysed via nitrogen cavitation under 750 psi for 5 min using a Parr cell disruption bomb. In a two-step centrifugation, lysate was spun at 500×*g* for 10 min at 4°C and collected supernatant was

spun at 13,000 RCF for 40 min at 4°C. Post-ultracentrifugation, the membrane-containing pellet was resuspended in TME buffer (25mM Tris-HCl, 5 mM $MgCl_2$, and 1 mM EDTA, pH 7.4) containing 7% sucrose (w/v). The Bradford assay (Bradford, 1976) was used to determine protein concentration. Membrane aliquots were stored at -80°C until use.

2.3 Saturation Radioligand Binding.

At least nine concentrations of radiolabeled ligand (typically ranging from 0.23 nM to 37.60 nM) were used to determine B_{max} and K_d values of the receptors. 5 µg of membrane was incubated at 30°C for 60 min in a total assay volume of 200 µl TME buffer containing 0.1% fatty acid-free bovine serum albumin (BSA) using [^{3}H]CP55940 (150.2 Ci/mmol, Perkin Elmer Life Sciences, Boston, MA). Nonspecific binding was determined with 1 µM unlabeled CP55940.

2.4 Radioligand Binding.

In heterologous competition binding experiments to determine K_i values of the receptor for the compound, 5-10 µg of CB_1 or CB_2 membrane were incubated for 60 min at 30°C with [^{3}H]CP55940 (150.2 Ci/mmol, Perkin Elmer Life Sciences, Boston, MA) at 1.5 nM, near the K_d value determined from saturation binding isotherms, in a total assay volume of 200 µl of TME buffer containing 0.1% BSA. Binding assays were performed using nine concentrations of unlabeled competitor test compound, typically from 100 pM to 100 µM. Unlabeled CP55940 at a concentration of 1 µM was used to determine nonspecific binding. Reactions were terminated upon addition of 300 µl TME buffer containing 5% BSA and filtration with a Brandel cell harvester through Whatman GF/C filter paper (Brandel, Gaithersburg, MD). Radioactivity trapped in filters was measured via liquid scintillation counting. When possible, total assay volume and amount of membrane were adjusted to avoid ligand depletion by keeping total bound ligand less than 10%.

2.5 Guanosine 5'-O-(3-Thio)Triphosphate (GTPγS) Binding.

In [^{35}S]GTPγS binding experiments, 8 µg of CB_2 membrane were incubated for 60 min at 30°C in a total assay volume of 200 µl of GTPγS binding buffer (50 mM Tris-HCl, pH 7.4,

3 mM $MgCl_2$, 0.2 mM EGTA, and 100 mM NaCl) with nine concentrations of test compound, 0.1 nM [^{35}S] GTPγS (1250 Ci/mmol, Perkin Elmer Life Sciences, Boston, MA), 10 μM GDP, and 0.1% (w/v) BSA. Unlabeled GTPγS at a concentration of 10 μM was used to determine nonspecific binding. Reactions were terminated via Whatman filtration. Bound [^{35}S]GTPγS trapped in filters was determined by liquid scintillation counting.

2.6 Immunoblotting Studies for ERK1/2 Phosphorylation.

HEK293T cells seeded in 6-well plates at a density of 2.0×10^5 cells per well and transiently expressing CB_1 or CB_2 were treated with 10 ng/mL pertussis toxin (PTX) (EMD Millipore Corporation, Billerica, MA) to abrogate $G_{i/o}$ protein signaling at 37°C prior to compound treatment. After 16 hours, cells were exposed to test compounds diluted in Gibco Opti-MEM reduced serum medium (Thermo Fisher Scientific, Rockford, IL) supplemented with 0.1% FBS for 5 minutes. Cells were then washed in ice-cold lysis buffer containing 150 mM NaCl, 1.0% IGEPAL CA-360, 0.5% sodium deoxycholate, 0.1% SDS, 50 mM Tris, pH 7.5, and protease inhibitor cocktail. Cell lysates were centrifuged at 18,000 RCF for 15 min at 4°C. After heating for 3 min at 95°C, 13 μg of total protein samples were resolved by 10% sodium dodecyl sulfate polyacrylamide gel electrophoresis (SDS-PAGE) run at 120V and were subsequently transferred to polyvinylidene fluoride (PVDF) membranes. After overnight incubation with SuperBlock T20 PBS blocking buffer (Fisher Scientific, Pittsburgh, PA), the membranes were incubated at RT with primary antibody (1:3000 anti-rabbit phospho-p44/42; Cell Signaling Technology, Danvers, MA) for 1 hour, then were washed with Tween-TBS (10X TBS and 0.1% Tween) for 10 min per wash for a total of three washes at RT. After secondary incubation with 1:6000 goat anti-rabbit peroxidase-conjugated antibody (Cell Signaling Technology, Danvers, MA) for 1 hour at RT on an orbital shaker, specific immunoreactivity was visualized using the Supersignal West Femto Chemiluminescent Substrate System (Thermo Fisher Scientific, Rockford, IL).

2.7 Data Analysis and Image Quantification.

All radioligand binding assays were carried out in triplicate (duplicate in parallel), with data presented as the mean ± SE value or the mean with corresponding 95% confidence limits from at least three independent experiments except when no binding was detected reproducibly. K_d and B_{max} values were calculated by nonlinear regression fitted to a one binding site model using GraphPad Prism 5.04 (GraphPad Software, La Jolla, CA). K_i values were calculated using the Cheng-Prusoff equation (Cheng and Prusoff, 1973) based on K_d values obtained from saturation binding isotherms.

Immunoreactive bands of phospho-ERK1/2 were quantified using the gel analysis tool in the open source software ImageJ/FIJI (National Institutes of Health, Bethesda, MD; https://imagej.nih.gov/ij/). pERK 1/2 band intensities are expressed as mean fold change over DMSO treatment for two independent experiments. A representative image is shown.

3. RESULTS

Chemical structures of test compounds pursued in greater detail at the molecular and cellular levels are summarized in Figure 8.

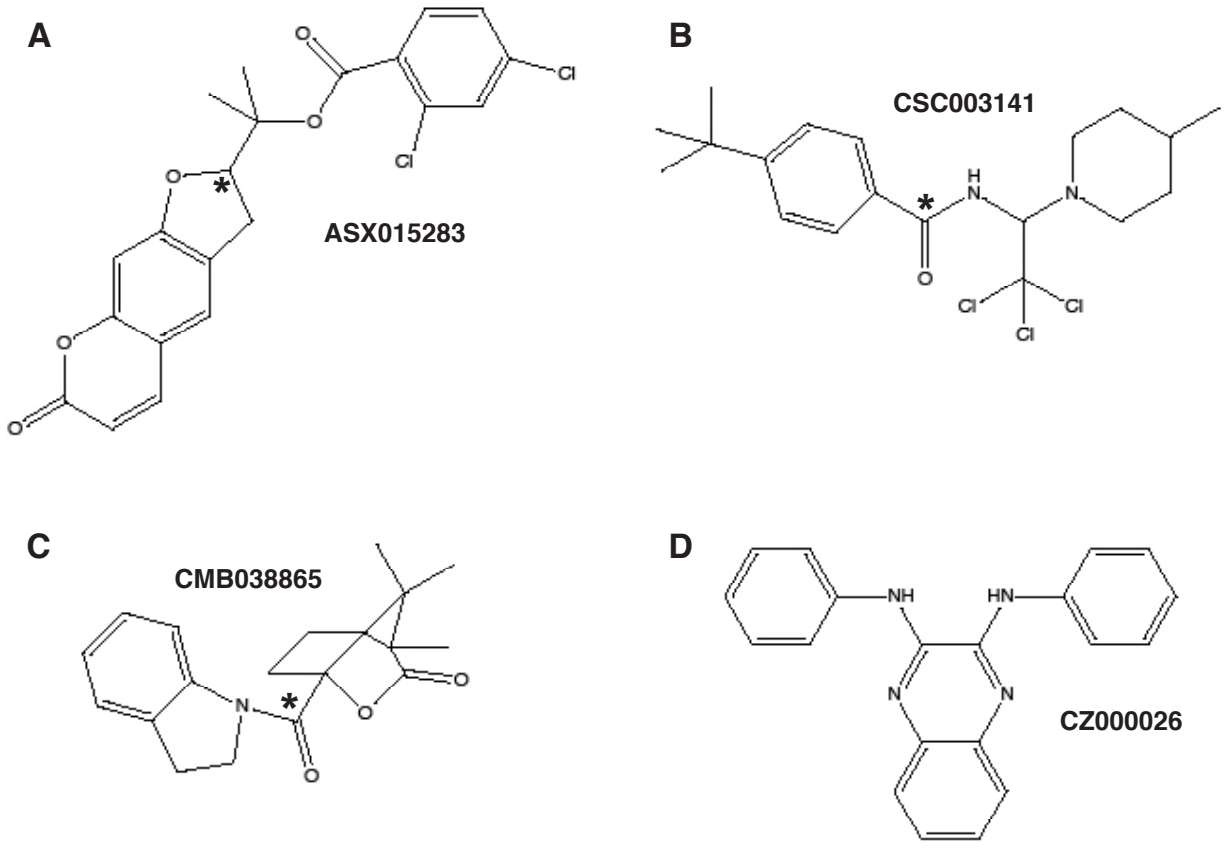

Figure 8. Putative CB_2-selective agonists. (A) ASX015283, (*2-(7-oxo-2,3-dihydro-7H-furo[3,2-g]chromen-2-yl)propan-2-yl 2,4-dichlorobenzoate*), MW 419.265 g/mol, (B) CSC003141, (*4-(tert-butyl)-N-(2,2,2-trichloro-1-(4-methylpiperidin-1-yl)ethyl) benzamide*), MW 405.799 g/mol, (C) CMB038865, (*1-(indoline-1-carbonyl)-4,7,7-trimethyl-2-oxabicyclo[2.2.1]heptan-3-one*), MW 299.370 g/mol, and (D) CZ00026, (*N2,N3-diphenylquinoxaline-2,3-diamine*), MW 312.376. * denotes chiral center.

3.1 Saturation binding isotherms.

Multiple saturation assays were performed throughout the experimental process of assessing test compound affinity for CB_1 and CB_2. Stoichiometry of receptor to G protein must be ensured upon creation of each new membrane preparation. Additionally, saturation binding assays serve as a preliminary measure to verify membrane preparation functionality and quality. B_{max} and K_d values are parameters of saturation binding isotherms. While B_{max} provides the maximum number of binding sites, K_d, the equilibrium binding constant, or concentration of ligand that is required to obtain half-maximum

binding of the receptor at equilibrium, indicates the affinity of the receptor for the radioligand [^{3}H]CP55940. A representative saturation binding assay performed with CB_2 membrane preparation is shown in Figure 9.

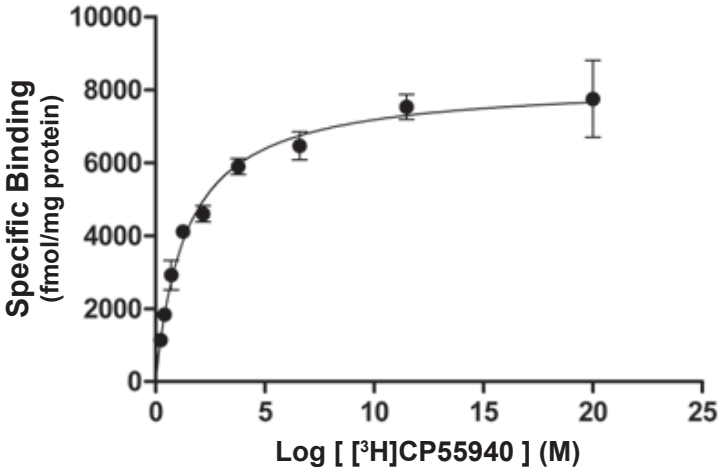

Figure 9. The equilibrium dissociation constant, K_d = 1.4 nM, of the known CB_2 agonist [^{3}H]CP55940 was directly determined in a saturation binding assay. Data is shown as mean of one independent experiment (duplicates performed in parallel).

3.2 ASX015283 and CSC003141 exhibit preferential binding to CB_2.

Based on heterologous competition binding experiments using radiolabeled [^{3}H]CP55940, test compounds ASX015283 and CSC003141 bind preferentially to CB_2 over CB_1. No concentration-dependent binding to CB_1 was detected up to 1 μM for both ASX015283 and CSC003141(Figures 10A and 11A).

For CB_2, as the concentration of ASX015283 and CSC003141 increases, these test compounds, ASX015283 and CSC003141, are able to outcompete radiolabeled CP55940 for the orthosteric binding site on CB_2, eliciting a decrease in specific binding

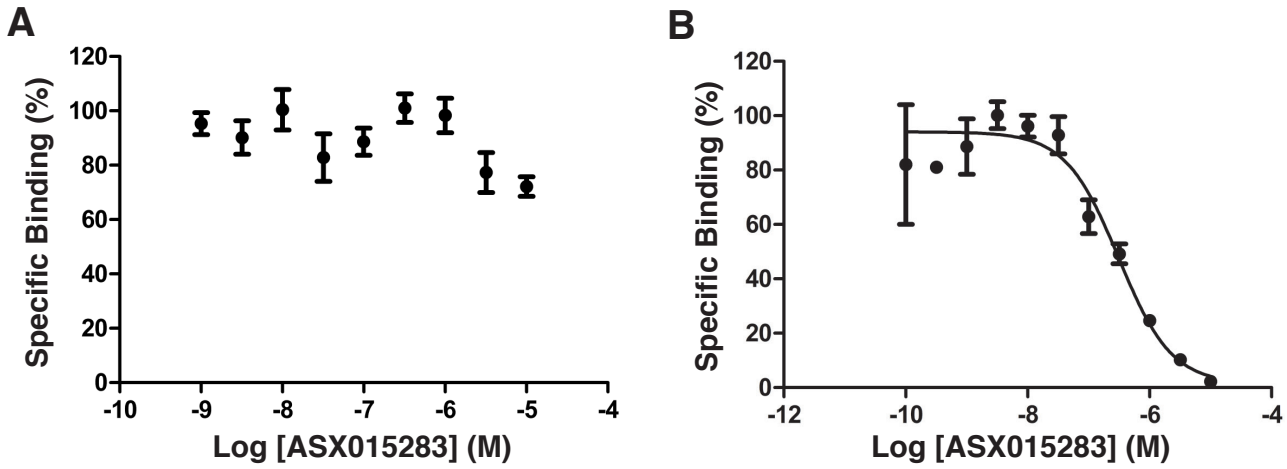

Figure 10. ASX015283 does not bind CB_1 up to 1 μM (A), however it binds CB_2 with K_i = 147 nM (B), as determined by competition radioligand binding assays against known agonist [^{3}H]CP55940. Data is depicted as the mean of three independent experiments, each performed in duplicate.

of CP55940. However, ASX015283 binds CB_2 with marginally stronger affinity compared to CSC003141 (i.e. ~1.6-fold; compare Figures 10B and 11B). ASX015283 binds CB_2 with an equilibrium dissociation constant K_i = 147 nM compared to CSC003141, with K_i = 242 nM. The difference in affinity between the two compounds is telling, however, not statistically significant. Since there is no CB_1 binding for these compounds, these compounds have a stronger binding affinity for CB_2 rather than CB_1. Therefore, ASX015283 and CSC003141 are selective for CB_2. Due to enhanced receptor subtype preference, these compounds were pursued further by assessing G protein coupling in GTPγS binding assays (refer to section 3.5).

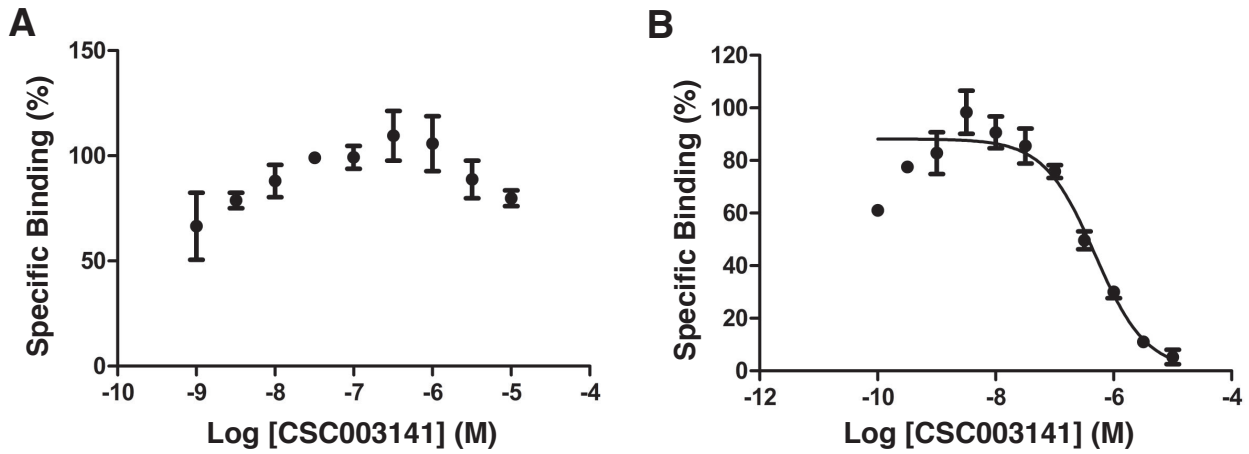

Figure 11. CSC003141 does not bind CB_1 up to 1 µM (A), however it binds CB_2 with K_i = 242 nM (B) as determined by competition radioligand binding assays against known agonist [^{3}H]CP55940. Data is depicted as the mean of three independent experiments, each performed in duplicate.

3.3 CMB038865 exhibits nearly 100X selectivity for CB_1.

Heterologous competition binding assays using radiolabeled [^{3}H]CP55940 with competitor test compound CMB038865 reveal that while CMB038865 does bind CB_2, it is approximately 100-fold more selective for CB_1.

CMB038865 binds to CB_2 in the high nanomolar range, with a K_i = 903 nM. CMB038865 binds to the CB_2 receptor with less potency compared to the interaction at CB_1. Although CMB038865 is a weak agonist for CB_2, it is not selective for the receptor, since CMB038865 also detectably binds CB_1. Binding to CB_1 is a higher affinity interaction, with K_i = 10 nM when analysis was done using the one site fit model. However, an increase in

specific binding of [^{3}H]CP55940, indicative of enhanced receptor activation, is consistent with that expected of positive allosteric modulation. Given the distinct and unexpected shape of the CB_1 binding curve with CMB038865 (Figure 12A), a one site binding model is inappropriate. An allosteric modulator titration model for the curve provides a K_B of 35 nM and α of 2.3.

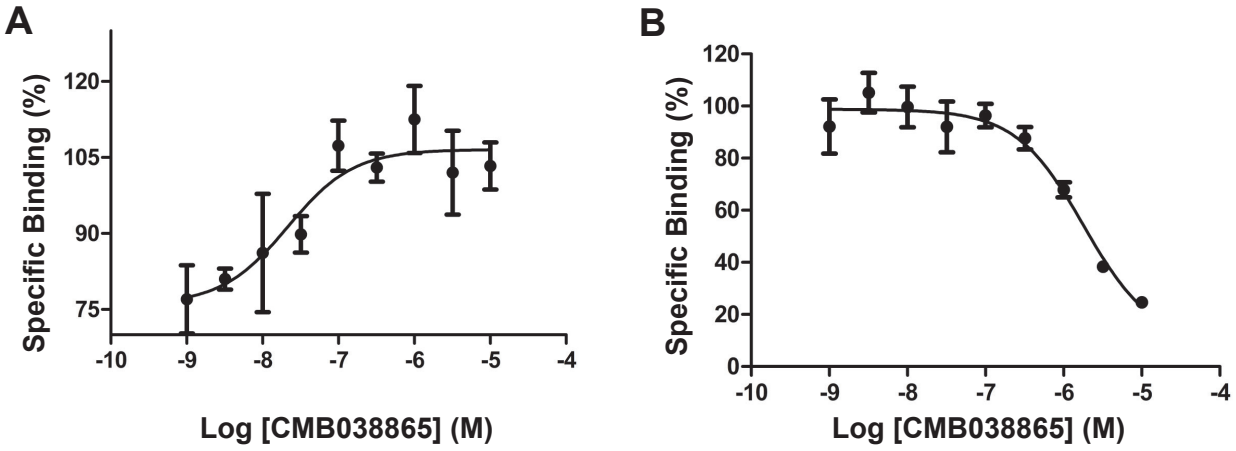

Figure 12. CMB038865 binds CB_1 with a K_B= 35 nM and α = 2.3, (A), and CB_2 with a K_i = 903 nM (B), as determined by competition radioligand binding assays against known agonist [^{3}H]CP55940. Data is depicted as the mean of three independent experiments, each performed in duplicate.

3.4 CZ000026 does not exhibit receptor subtype selectivity.

Heterologous competition binding experiments with radiolabeled [^{3}H]CP55940 were performed with test compound CZ000026. CZ000026 has low affinity for both CB_1 and CB_2, binding both receptors in the micromolar range. The equilibrium dissociation constant for CB_1 binding, K_i = 1.8 μM (1798 nM), is indicative of a weak binding interaction. The compound binds to CB_2 with similar affinity, with K_i = 1.1μM (1097 nM). Compared to test compounds ASX015283, CSC003141, and CMB038865, which are selective for either CB_1 or CB_2, CZ000026 is neither selective nor particularly potent at either receptor. All binding data for these test compounds is summarized in Table 1.

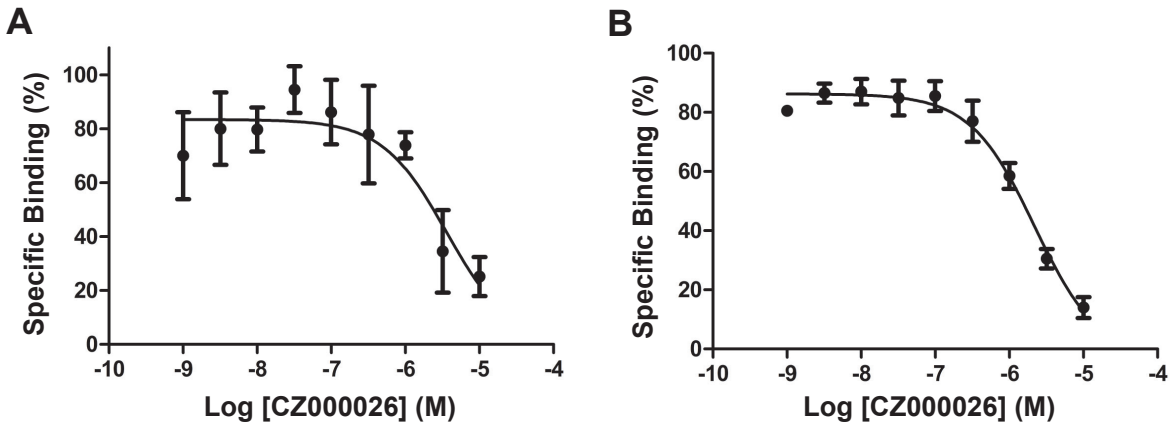

Figure 13. CZ000026 binds CB_1 with K_i = 1796 nM (A), and CB_2 with K_i = 1097 nM (B), as determined by competition radioligand binding assays against known agonist [^{3}H]CP55940. Data is depicted as the mean of three independent experiments, each performed in duplicate.

Table 1. Test compound binding to CB_1 and CB_2 using [^{3}H]CP55940 as a tracer.

			K_i (nM)	
	K_B (nM)	α	CB_1	CB_2
ASX015283*			N.B.[a]	147
CSC003141*			N.B.[a]	242
CMB038865*	35	2.3	“10”	903
CZ000026			1796	1097

[a] no binding detected up to 1 μM
* enantiomeric mixture

3.5 Dose-dependent GTPγS binding is elicited by all test compounds.

[^{35}S]GTPγS radioligand binding assays were performed on all test compounds to evaluate G protein coupling activity as a result receptor activation elicited by test compound binding. This functional assay monitors G protein activation by determining the extent of binding nonhydrolyzable GTP analog to Gα subunits. G protein activation was initially implicated in inhibition of cAMP accumulation assays conducted by Bristol-Myers Squibb, with EC_{50} values shown in Table 2, as expected for a G_i coupled GPCR. Additionally, three of the four compounds are agonists at CB_2, albeit to varying extents of agonism, with binding affinities summarized in Table 1.

Table 2. [^{35}S]GTPγS binding of test compounds at CB_2.

Ligand	EC_{50} (nM)	
	cAMP[a]	GTPγS[b]
ASX015283*	73	57
CSC003141*	29	78
CMB038865*	45	105
CZ000026	45	620

[a] inhibition of cAMP accumulation in high throughput screens; [b] binding of radiolabeled [^{35}S] GTPγS;* enantiomeric mixture.

All four test compounds elicited a dose-dependent increase in specific GTPγS binding upon activation of CB_2, with EC_{50} values in the nanomolar range. ASX015283 robustly activated G protein coupling, with EC_{50} = 57 nM. CSC003141 also caused an increase in activated G protein binding, with EC_{50} = 78 nM. CMB038865 had an EC_{50} = 105 nM. Test compound CZ000026 was least effective at eliciting the dose-dependent increase in specific GTPγS binding, with an EC_{50} value of 620 nM. In general, test compounds ASX015283, CSC003141, and CMB038865 were more efficacious in their ability to activate G protein subunits compared to CZ000026. These data are summarized in Table 2.

3.6 Extracellular signal-regulated kinase phosphorylation studies.

Two test compounds, ASX015283 and CMB038865, with high affinity for CB_2 or CB_1 respectively, were pursued further to assess downstream signaling via the mitogen-activated protein kinase (MAPK) pathway as measured by the phosphorylation of isoforms of extracellular signal-regulated kinase (ERK).

ERK was selected to assess downstream signaling due to its robust signal upon compound-induced receptor activation. This high signal, along with spatiotemporal factors, facilitates the differentiation of G protein or β-arrestin-mediated signaling. To confirm $G_{i/o}$ protein-dependent ERK phosphorylation, pertussis toxin (PTX) was used to abrogate $G_{i/o}$ and determine if that diminishes downstream phosphorylation of ERK. PTX blocks G protein signaling via G_i, resulting in lower levels of ERK phosphorylation, as shown in Figures 15 and 17.

ASX015283 induces robust ERK phosphorylation. At a 0.1 μM concentration of ASX015283, ERK phosphorylation was nearly 12-fold higher than basal level DMSO treatment (Figure 15). This concentration of ASX015283 provided the highest level of ERK phosphorylation and therefore is the optimal effective concentration of the test compound for treatment with minimal cytotoxicity. Since treatment with test compound ASX015283 in the presence of PTX abrogated ERK phosphorylation, ASX015283 initiates $G_{i/o}$ protein-dependent phosphorylation of this downstream kinase.

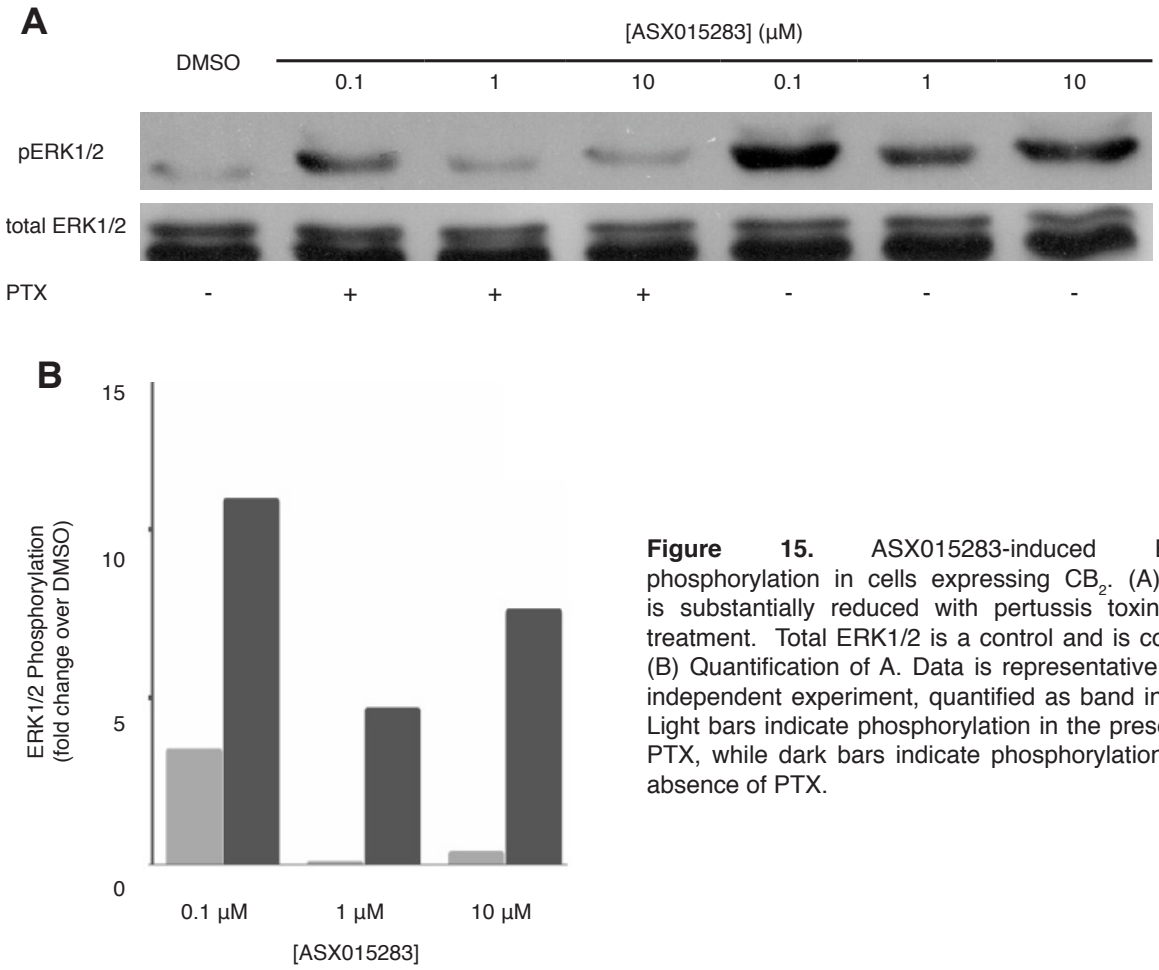

Figure 15. ASX015283-induced ERK1/2 phosphorylation in cells expressing CB_2. (A) pERK is substantially reduced with pertussis toxin (PTX) treatment. Total ERK1/2 is a control and is constant. (B) Quantification of A. Data is representative of one independent experiment, quantified as band intensity. Light bars indicate phosphorylation in the presence of PTX, while dark bars indicate phosphorylation in the absence of PTX.

CMB038865, with nearly 100-fold selectivity for CB_1 over CB_2, also engages in robust phosphorylation of ERK. However, robust phosphorylation is only induced by CB_2 activation. In CB_1-expressing cells, PTX does not affect CMB03885-induced ERK phosphorylation (Figure 16) and levels of ERK phosphorylation are low across both concentrations of test compound. However, in CB_2-expressing cells, PTX significantly

reduces ERK signal to nearly basal levels. At a 0.5 μM concentration of CMB038865 in cells expressing CB_2, ERK phosphorylation levels are approximately 100-fold higher than basal level (Figure 17). Given the binding affinity for CMB038865 at CB_2 (K_i = 903 nM), this level of phosphorylation is particularly remarkable considering this concentration of test compound elicits less than half receptor occupancy. All binding and downstream signaling data for these test compounds are summarized in Table 3.

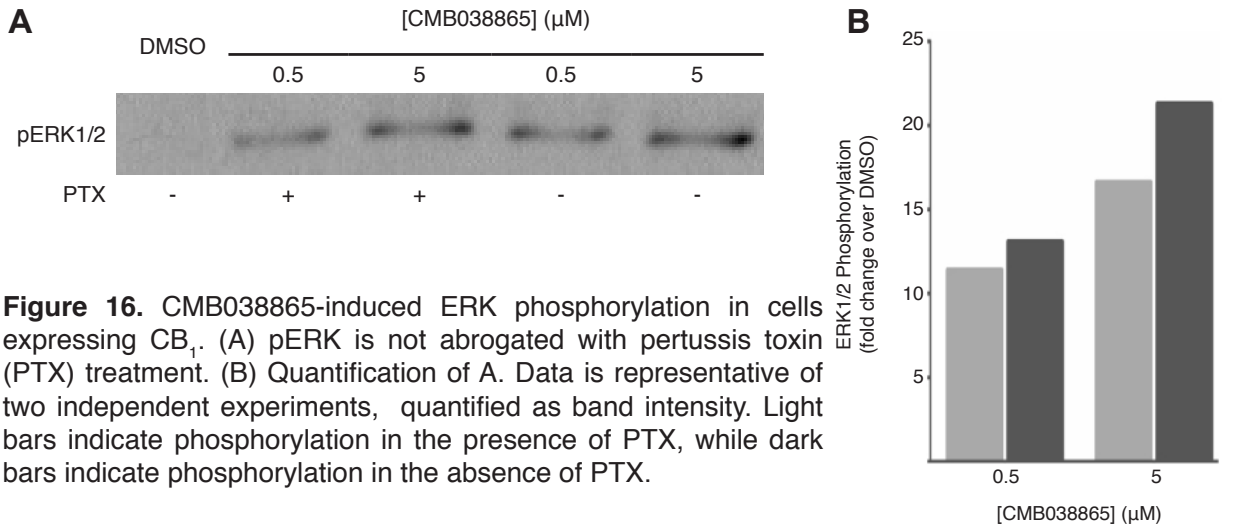

Figure 16. CMB038865-induced ERK phosphorylation in cells expressing CB_1. (A) pERK is not abrogated with pertussis toxin (PTX) treatment. (B) Quantification of A. Data is representative of two independent experiments, quantified as band intensity. Light bars indicate phosphorylation in the presence of PTX, while dark bars indicate phosphorylation in the absence of PTX.

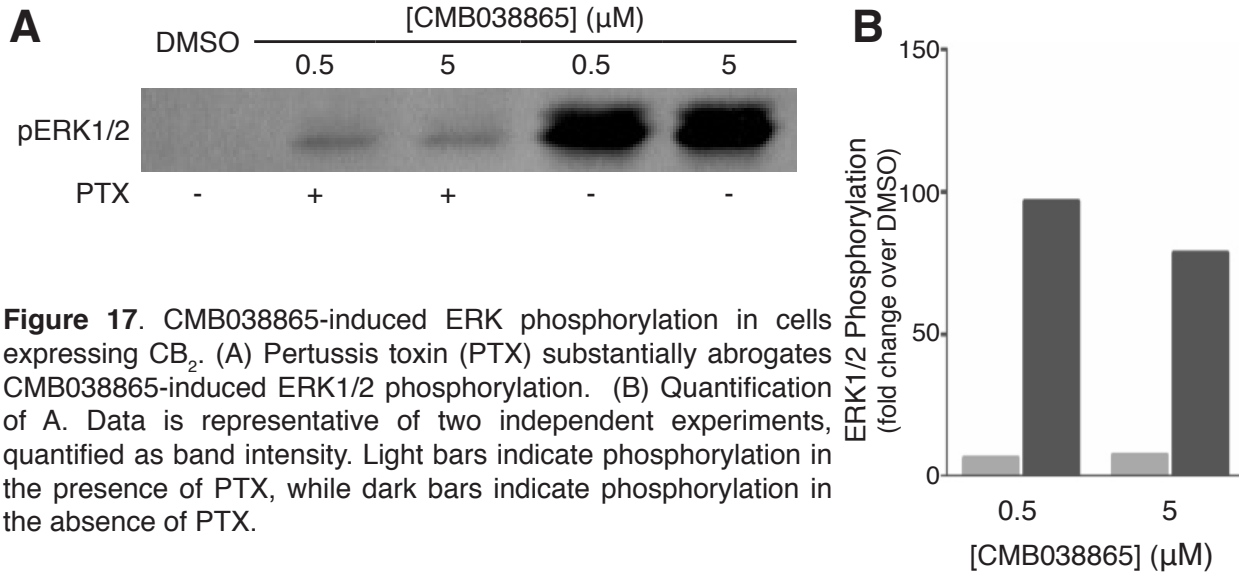

Figure 17. CMB038865-induced ERK phosphorylation in cells expressing CB_2. (A) Pertussis toxin (PTX) substantially abrogates CMB038865-induced ERK1/2 phosphorylation. (B) Quantification of A. Data is representative of two independent experiments, quantified as band intensity. Light bars indicate phosphorylation in the presence of PTX, while dark bars indicate phosphorylation in the absence of PTX.

Table 3. Summary of radioligand binding, GTPγS binding, and ERK phosphorylation studies.

	K_i (nM)		GTPγS binding EC_{50} (nM)	PTX-sensitive ERK phosphorylation	
Ligand	CB_1	CB_2	CB_2	CB_1	CB_2
ASX015283*	N.B.[a]	147	57	N.D.[b]	+
CSC003141*	N.B.[a]	242	78	N.D.[b]	N.D.[b]
CMB038865*	10[c]	903	105	-	++
CZ000026	1796	1097	620	N.D.[b]	N.D.[b]

* enantiomeric mixture; [a] No binding detected up to 1 μM; [b] Assay not done for the indicated ligand and receptor combination; [c] One site fit binding model (allosteric model provides K_b = 35 nM.)

4. DISCUSSION

These data indicate that of the four structurally distinct putative CB_2-selective agonists investigated in this study, ASX015283 and CSC003141 are selective agonists of CB_2 that do not detectably interact with CB_1 up to 1 μM. ASX015283 is more potent than CSC003141 at binding the orthosteric site of CB_2. However, while the ~ 1.6-fold difference between the binding affinity at CB_2 for these two compounds (K_i = 147 nM vs. 242 nM) is telling, it is not statistically significant (p = 0.100), as determined by the Mann-Whitney non-parametric t-test (Mann and Whitney, 1947).

As a result of their activation of CB_2, these compounds also are effective at inducing receptor coupling to G protein subunits. ASX015283, the compound with the strongest affinity interaction at the CB_2 receptor level and most potent inducer of G protein coupling (Figure 14A), engages in downstream signaling as determined by 5-minute test compound-induced PTX-sensitive phosphorylation of ERK ½ isoforms.

CZ00026 binds both receptors with weak affinity within the micromolar range. Therefore, CZ00026 is a non-preferential weak agonist of CB_1 and CB_2. Despite weak binding affinity, this compound sufficiently activates CB_2 to induce G protein coupling within the nanomolar range as determined by GTPγS assays. However, due to lack of receptor subtype selectivity and weak binding affinity, this compound will not be pursued in further studies.

CMB038865 binds CB_2 at high nanomolar (K_i = 903 nM) affinity, indicating a relatively weak binding interaction of the test compound with the receptor. Surprisingly, in competition radioligand binding assays, CMB038865 binds CB_1 with strong affinity (K_i = 10 nM; K_B = 35 nM) but does not inhibit CP55940 binding as expected of an agonist. Rather, CMB038865 enhances specific binding of CP55940 in a dose-dependent manner. This finding is consistent with that of positive allosteric modulation. A plausible mechanism is that CMB038865 acts at a topographically distinct allosteric site on CB_1 to

enhance the binding of the ligand at the orthosteric site. Therefore, CMB038865 is a weak agonist at CB_2, and a putative PAM for CB_1. These suspected properties of CMB038865 make it a rare addition to the pharmacological toolkit available to the field.

Activation of CB_2 by CMB038865 resulted in receptor coupling of G protein subunits as determined by GTPγS binding assays. Additionally, CMB038865 induced robust ERK phosphorylation in cells expressing CB_2, with a nearly 100-fold increase over vehicle treatment. This is remarkable in terms of efficacy since at a concentration of 0.5 μM, robust ERK ½ phosphorylation was elicited with less than half receptor occupancy. PTX markedly diminishes ERK signal in CB_2 expressing cells, but not in CB_1- expressing cells. Upon CMB038865-induced activation of CB_1, ERK phosphorylation levels remain consistently low regardless of the presence of PTX. To ensure that these results were not due to the presence of CMB038865 as a metabolite, new drug stocks were prepared before each experiment. As PTX abrogates $G_{i/o}$ signaling, it is plausible that this compound engages in alternative downstream signaling mechanisms when interacting with CB_1 or does not go through ERK pathways.

As chronic pain remains a common affliction of American adults, drug discovery efforts have shifted priority to an avenue of non-addictive, non-opioid analgesic and anti-inflammatory agents. By selectively targeting CB_2, analgesia is possible without the psychoactive effects of CB_1 activation in the central nervous system. However, achieving receptor subtype selectivity is a pharmacological feat, given that the orthosteric binding site is largely conserved across cannabinoid receptor subtypes. ASX015283 and CSC003141 are able to surmount this difficulty by selectively targeting CB_2.

Due to the enantiomeric nature of both CB_2-selective compounds, ASX015283 and CSC003141, as well as the putative CB_1 PAM CMB038865, separation of the compounds into individual enantiomers would be of potential clinical benefit. Enantiopure forms of compounds have been shown to potentially act antagonistically towards each other. One novel allosteric modulator for CB_1, GAT211, when separated into its chiral forms had

agonist activity in the R-(+)-enantiomer (GAT 228) and PAM activity with the S-(-)-enantiomer (GAT 229) (Laprairie et al., 2017). Separation of test compounds into enantiomeric forms will be pursued via asymmetric synthesis or chiral chromatography. Enantiopure compounds will then be characterized using these assays and others if they show promise in initial screens.

Once enantiopure forms have been obtained, to further pursue these leads, structure-activity relationship studies will be conducted on ASX015283, the compound with strongest affinity for CB_2 within the nanomolar range, as well as the putative PAM, CMB038865. Modifications to the structural scaffolds will be performed by collaborator of the Kendall laboratory, Dr. Dai Lu of Texas A&M Rangel College of Pharmacy, to enhance the binding affinity of the test compound to CB_2 within lower nanomolar or optimally sub-nanomolar ranges.

Additionally, an interesting pursuit for these compounds would be to obtain a holistic phosphorylation profile. Future studies will include measuring levels of phosphorylation of other kinases, including Src and Jnk. To assess analgesic and anti-inflammatory properties of these compounds, studies examining the levels of mRNA expression of CB_2 in addition to other markers of pain, as well as patterns in immune cell migration, and animal studies will be performed.

In summary, the chief finding of this study is that ASX015283 and CSC003141 are CB_2-selective orthosteric agonists with reasonably high affinity. While CMB038865, a weak agonist at CB_2, binds to CB_1 with at least 100-fold enhanced binding affinity, and is consistent with a positive allosteric modulator acting at CB_1 due to its ability to increase specific binding of orthosteric ligand CP55940.

The pharmacological profile of ASX015283 and CSC003141 as receptor subtype selective compounds offers promising potential therapeutic advantages in the case of treating chronic pain and inflammatory conditions. These leads serve as the starting point

for the development of small molecule agonists with enhanced potency at CB_2 for optimal analgesic and anti-inflammatory effects in the absence of psychotrophic interactions.

REFERENCES

Amenta PS, Jallo JI, Tuma RF, Hooper DC and Elliott MB (2014) Cannabinoid receptor type-2 stimulation, blockade, and deletion alter the vascular inflammatory responses to traumatic brain injury. *J Neuroinflammation* **11**:191.

Bradford MM (1976) A rapid and sensitive method for the quantitation of microgram quantities of protein utilizing the principle of protein-dye binding. *Anal Biochem* **72**: 248-254

Chen C and Okayama H (1987) High-efficiency transformation of mammalian cells by plasmid DNA. *Mol Cell Bio* **7**: 2745-2752.

Cheng Y and Prusoff WH (1973) Relationship between the inhibition constant (K_i) and the concentration of inhibitor which causes 50 per cent inhibition (I_{50}) of an enzymatic reaction. *Biochem Pharmacol.* **22**: 3099–108

Erdozain AM, Diez-Alarcia R, Meana JJ and Callado LF (2012) The inverse agonist effect of rimonabant on G protein activation is not mediated by the cannabinoid CB1 receptor: evidence from postmortem human brain. *Biochem Pharmacol* **83**:260-268.

Gilchrist A (2010) GPCR molecular pharmacology and drug targeting shifting paradigms and new directions. Wiley, Hoboken, NJ.

Houze J, McKendry S, Gergely J, Xia Y, Shan B, Kayser F. U.S. Patent 7,511,043. 2009.

Ishii T, Muranaka R, Tashiro O and Nishimura M (2007) Chronic intracerebroventricular administration of anti-neuropeptide Y antibody stimulates starvation-induced feeding via compensatory responses in the hypothalamus. *Brain Res* **1144**:91-100.

Laprairie RB, Kulkarni PM, Deschamps JR, Kelly ME, Janero DR, Cascio MG, Stevenson LA, Pertwee RG, Kenakin TP, Denovan-Wright EM and Thakur GA (2017) Enantiospecific Allosteric Modulation of Cannabinoid 1 Receptor. *ACS Chem Neurosci*.

Lin R, Elf S, Shan C, Kang HB, Ji Q, Zhou L, Hitosugi T, Zhang L, Zhang S, Seo JH, Xie J, Tucker M, Gu TL, Sudderth J, Jiang L, Mitsche M, DeBerardinis RJ, Wu S, Li Y, Mao H, Chen PR, Wang D, Chen GZ, Hurwitz SJ, Lonial S, Arellano ML, Khoury HJ, Khuri FR, Lee BH, Lei Q, Brat DJ, Ye K, Boggon TJ, He C, Kang S, Fan J and Chen J (2015) 6-Phosphogluconate dehydrogenase links oxidative PPP, lipogenesis and tumour growth by inhibiting LKB1-AMPK signalling. *Nat Cell Biol* **17**:1484-1496.

Mann HB and Whitney DR (1947) On a Test of Whether one of Two Random Variables is Stochastically Larger than the Other. *Ann Math Statist* **18**: 50-60.

Matucci R, Nesi M, Martino MV, Bellucci C, Manetti D, Ciuti E, Mazzolari A, Dei S, Guandalini L, Teodori E, Vistoli G and Romanelli MN (2016) Carbachol dimers as homobivalent modulators of muscarinic receptors. *Biochem Pharmacol* **108**:90-101.

Mikasova L, Groc L, Choquet D and Manzoni OJ (2008) Altered surface trafficking of presynaptic cannabinoid type 1 receptor in and out synaptic terminals parallels receptor desensitization. *Proc Natl Acad Sci U S A* **105**:18596-18601.

Nettekoven M, Fingerle J, Grether U, Gruner S, Kimbara A, Pullmann B, Rogers-Evans M, Rover S, Schuler F, Schulz-Gasch T and Ullmer C (2013) Highly potent and selective cannabinoid receptor 2 agonists: initial hit optimization of an adamantyl hit series identified from high-through-put screening. *Bioorg Med Chem Lett* **23**:1177-1181.

Persidsky Y, Fan S, Dykstra H, Reichenbach NL, Rom S and Ramirez SH (2015) Activation of Cannabinoid Type Two Receptors (CB2) Diminish Inflammatory Responses in Macrophages and Brain Endothelium. *J Neuroimmune Pharmacol* **10**:302-308.

Pertwee RG (2008) The diverse CB1 and CB2 receptor pharmacology of three plant cannabinoids: delta9-tetrahydrocannabinol, cannabidiol and delta9-tetrahydrocannabivarin. *Br J Pharmacol* **153**:199-215.

Rosenbaum DM, Rasmussen SG and Kobilka BK (2009) The structure and function of G-protein-coupled receptors. *Nature* **459**:356-363.

Rosselli S, Maggio AM, Faraone N, Spadaro V, Morris-Natschke SL, Bastow KF, Lee KH and Bruno M (2009) The cytotoxic properties of natural coumarins isolated from roots of Ferulago campestris (Apiaceae) and of synthetic ester derivatives of aegelinol. *Nat Prod Commun* **4**:1701-1706.

Sepe V, Festa C, Renga B, Carino A, Cipriani S, Finamore C, Masullo D, Del Gaudio F, Monti MC, Fiorucci S and Zampella A (2016) Insights on FXR selective modulation. Speculation on bile acid chemical space in the discovery of potent and selective agonists. *Sci Rep* **6**:19008.

Shore DM and Reggio PH (2015) The therapeutic potential of orphan GPCRs, GPR35 and GPR55. *Front Pharmacol* **6**:69.

Turu G and Hunyady L (2010) Signal transduction of the CB1 cannabinoid receptor. *J Mol Endocrinol* **44**:75-85.

Whalen EJ, Rajagopal S and Lefkowitz RJ (2011) Therapeutic potential of beta-arrestin- and G protein-biased agonists. *Trends Mol Med* **17**:126-139.

Wootten D, Christopoulos A and Sexton PM (2013) Emerging paradigms in GPCR allostery: implications for drug discovery. *Nat Rev Drug Discov* **12**:630-644.